

# Coercive Force of Precipitation Alloys

A. H. GEISLER

*General Electric Research Laboratory, The Knolls, Schenectady, New York*

Cunco, Cunife, and the various types of Alnico are structurally analogous in that at the state of high coercive force the crystal structure of the precipitate is distorted from a cubic lattice to a tetragonal lattice. A single empirical relation has been derived from the data for these types of materials in which maximum coercive force is directly related to degree of tetragonality and saturation induction of the precipitate. On the basis of the fine particle theory this result suggests that not only shape anisotropy but also crystal anisotropy, as affected by strain, contributes to the coercive force. This work represents the first successful attempt to correlate the coercive force of the various commercial permanent magnet alloys with more fundamental characteristics.

THE energy of a magnetic material, as exhibited by the area under the demagnetization curve, increases directly with the three properties: residual induction, squareness of the loop, and coercive force. It would be desirable to relate these properties to more fundamental characteristics of the material. Although it seems that residual induction and squareness of the loop depend upon characteristics such as saturation induction, packing factor (ratio of ferromagnetic phase to total value), and orientation, the origin of coercive force has been somewhat more elusive. The coercive force of all permanent magnet alloys originates in a solid state transformation which is promoted by the heat treatment of these materials. The transformation proceeds by the nucleation and growth of a new phase within the parent matrix. The particles of the new phase are usually anisotropic in shape, frequently plate-like as in Fig. 1. Since the particles start from embryos of a few unit cells in size, they would be expected to grow

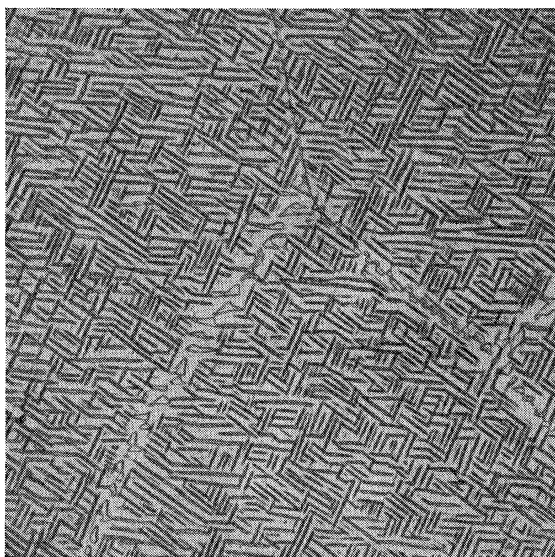


FIG. 1. Microstructure of Alnico 2 showing plate-like precipitate of resolvable particles larger than those responsible for high coercive force.  $1000\times$ .

during heat treatment through the size range where magnetic behavior is based on single domain particles. Thus, one would immediately expect that the fine particle theory derived for shape anisotropy would be applicable. In order to test this possibility, the coercive force of a variety of permanent magnet alloys is plotted in Fig. 2 against the saturation intensity estimated for the precipitates in these alloys. Both the packing factor and shape anisotropy are about the same for the alloys listed, and consequently, a direct proportionality would be expected between coercive force and saturation intensity. Since no simple relation is apparent in Fig. 2, an examination of the structural features of these alloys is essential in order to develop a good correlation with coercive force.

Three of the commercial permanent magnet alloys, namely, Alnico, Cunco, and Cunife, are cubic solid solutions which decompose into two cubic phases of slightly different lattice parameters during the aging heat treatment. This behavior occurs over a specific range of compositions in the Fe-Ni-Al, Cu-Ni-Co, and Cu-Ni-Fe systems upon which the alloys are based, respectively. The prototype of these alloys is the Ni-Au system, which will be used for simplicity in describing the characteristics of this class of materials. During the precipitation heat treatment the properties change as shown in Fig. 3. Saturation magnetization and remanence increase as the ferromagnetic nickel precipitate forms. On the other hand, the coercive force first increases and then decreases. At the condition of high coercive force the decomposition products are coherent with each other and thus have tetragonal crystal structures instead of cubic.<sup>1</sup> A possible role of the tetragonal structure will be developed subsequently.

An interpretation for the composition dependence of properties of diverse series of alloys will be more extensive than a postulate of high coercive force that is based upon a single alloy. Thus in the present work the principal concern will be given to explaining the variation in properties across the composition scale as in Fig. 4; the magnetic annealing of Alnico 5, which has adequately been explained as an orientation effect of the

<sup>1</sup> A. H. Geisler, *Trans. Am. Soc. Metals* **43**, 70 (1951).

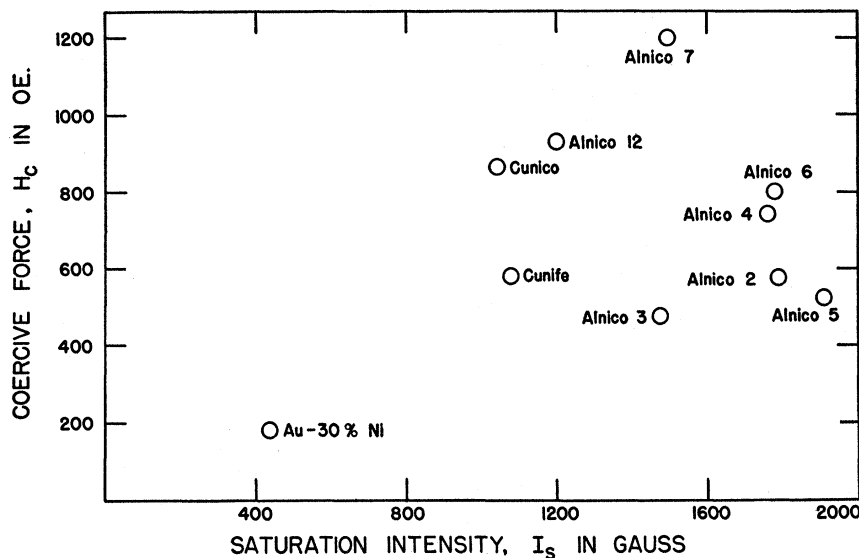


FIG. 2. Coercive force of various commercial alloys as related to intensity of magnetization at saturation of precipitate.

precipitate, will be neglected, and only properties for treatment without field will be considered. The variation in remanence in Fig. 4 is to be expected, since the induction increases as the amount of nickel in the alloy increases. On the other hand, the maximum coercive force from a curve such as in Fig. 3, when plotted against composition as in Fig. 4, increases continuously as the amount of nickel *decreases* when field strength is sufficient to saturate the alloy ( $H_{max}=1500$  oersteds or greater).\* The relationship appears to be general for the various alloy systems of the type considered here, in that the coercive force continuously increases as the ferromagnetic components of the alloy decrease within the composition range for heat-treatable alloys. The simplicity of the precipitation process in these alloy systems and the prototype Ni-Au permits an evaluation of the coherent state, relative to the fine particle theory, in explaining the variation of coercive force with alloy

composition. Theoretical relationships for the coercive force of fine precipitates have been derived from fundamental properties such as saturation magnetization, magnetostriction, and magnetic anisotropy constant.<sup>2</sup> It would be in order now to seek empirical relationships expressing the composition dependence of coercive force in the precipitation alloys, in order to evaluate the theoretical relationships.

The usual theorist has not had a very deep appreciation of the heterogeneous state of matter. This conclusion is evident by past treatments of order-disorder phenomena, in which little recognition has been provided for a two-phase equilibrium at temperatures between that for disorder and that for long-range order. Likewise, a heterogeneous mechanism of nucleation and growth of the ordered phase from the disordered, which has been identified and found useful in explaining the transient maximum in the coercive force during order-

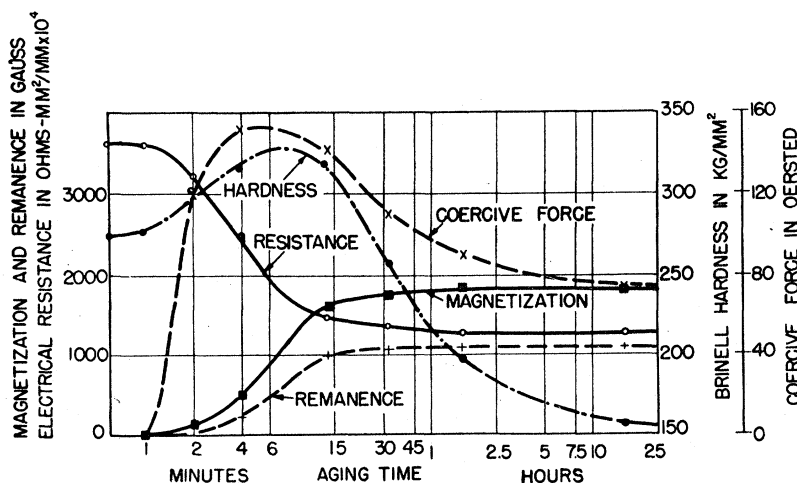


Fig. 3. Changes in properties of an Au-30 percent Ni alloy quenched from 900°C and aged designated intervals at 500°C. From Köster and Dannöhl (see reference 3).

\* The broken part of the curve at the left is probably imaginary, limited because the alloys are no longer ferromagnetic.  
<sup>2</sup> C. Kittel, *Revs. Modern Phys.* 21, 541 (1949).

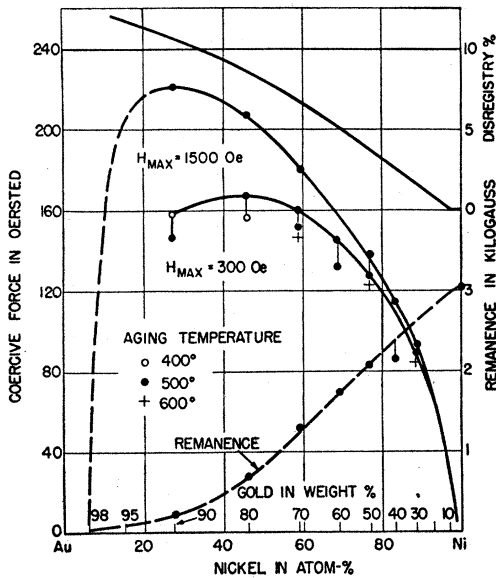


FIG. 4. Compositions dependence of maximum coercive force, remanence, and disregistry for Ni-Au alloys. From Köster and Dannöhl (see reference 3).

ing, was not provided for in theory. With no insight of the constitution of Ni-Au alloys, one might glibly conclude from Fig. 4 that these are alloys in which increasing coercive force with higher gold is associated with decreasing saturation intensity, increasing magnetostriction, or increasing magnetocrystalline anisotropy. In order to illustrate the types of information portrayed by the phase diagram and pertinent to an explanation of the composition dependence of magnetic properties, a brief description of the significance of the phase diagram follows.

Some features essential for an understanding of these alloys can be illustrated by Fig. 5, which represents schematically the phase diagram and lattice parameter variation for Ni-Au and also applies qualitatively to appropriate compositions in the ternary alloy systems. The miscibility gap in the solid solutions field is the basis for the heat treatment of these alloys. An alloy of composition X, when quenched from high temperatures and aged at  $T_1$ , decomposes into the two phases, of compositions  $C\alpha_1$  and  $C\alpha_2$  and appropriate lattice parameters. The weight fraction of each phase in the mixture at final equilibrium is given by the lever law from the sections of the tie line AC. For the nickel-rich phase  $\alpha_2$  the fraction is  $AB/AC$ . Regardless of alloy composition, in a series between  $C\alpha_1$  and  $C\alpha_2$  all heat-treatable alloys decompose at  $T_1$  into the same phases, of compositions  $C\alpha_1$  and  $C\alpha_2$ . Thus, bulk properties such as Curie temperature are those of the ferromagnetic phase, of composition  $C\alpha_2$ , and remain constant for the series of aged alloys. Consequently, direct variation of bulk properties such as saturation magnetization, magnetostriction, and magnetic anisotropy constants of the cubic ferromagnetic phase cannot be used to explain the

composition variation of coercive force (Fig. 4). On the other hand, the effect of changing composition from  $C\alpha_1$  to  $C\alpha_2$  is to change the relative amounts of the two phases at equilibrium according to the lever law as pointed out above. This mixing obviously accounts for the changing residual magnetization of the two-phase alloys, although the bulk properties of the ferromagnetic phase remain constant.

The phase diagram shows that at equilibrium, two features concerning the ferromagnetic phase  $\alpha_2$  change as the composition of the alloy is changed towards higher gold: first, the weight fraction of  $\alpha_2$  in the alloy decreases, and second, the composition and lattice parameter of the parent phase  $\alpha_x$  becomes more different from that of  $\alpha_2$ . The first feature expresses the ultimate packing factor for complete precipitation which should be considered in regard to the coercive force of fine particles as controlled by shape anisotropy. The second feature, when expressed as disregistry between the parent phase and the ferromagnetic precipitate (at top of Fig. 4), is related to the tetragonality which the lattice of the first particles to form must assume when they precipitate in the matrix. Both of these features change in the expected direction to explain the increasing coercive force with increasing gold content in the alloy.

The relationships between coercive force and the two features which possibly could be related to the variation with composition should now be examined. In Fig. 6 the ultimate packing factor by volume, which was obtained

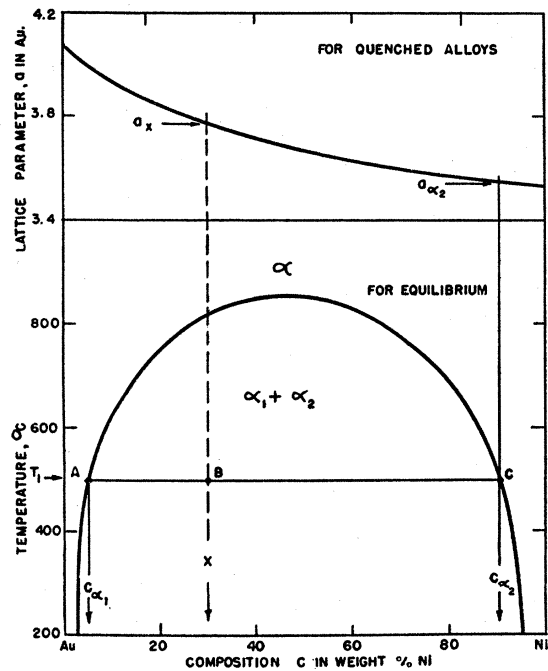
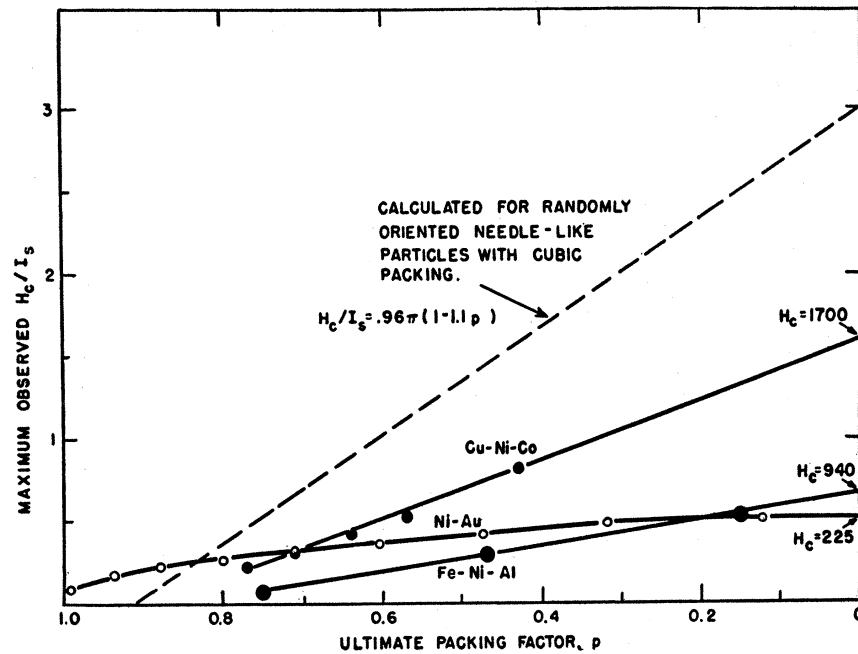


FIG. 5. Lattice parameter and miscibility gap in solid state of Ni-Au alloys.

FIG. 6. Composition dependence for shape anisotropy.



from the corresponding phase diagrams<sup>3-5</sup> and corrected for density, is plotted against the observed ratio  $H_c/I_s$  for three series of alloys.<sup>†6,7</sup> The maximum observed coercive force  $H_c$  was obtained from published data for the variation of  $H_c$  with time for different aging temperatures. The intensity of magnetization at saturation was obtained from published data corresponding to the composition of the precipitate as determined from the phase diagrams. The plotted data show little tendency to group into a single curve. Thus, another variable must be considered to give a general relationship for coercive force. Comparison of the observed data with calculated data will be discussed later.

The relationship between coercive force and disregistry is shown in Fig. 7. The disregistry values  $\delta$  were calculated from lattice parameter measurements for the supersaturated solid solutions<sup>1,3,8,9</sup> and equilibrium precipitates of compositions determined from the phase diagrams. When the quantities are plotted on logarithmic scales a straight line relationship results. This relation is particularly evident for the Ni-Au series, where most data were available. The data for the Cu-Ni-Co series were for maximum energy product, which appar-

ently does not occur under the same aging conditions as maximum coercive force in the two alloys of greatest disregistry. This condition explains the departure of the line from the two points at the upper end of the series. A second point is given for a disregistry of 0.7 which is the maximum  $H_c$  of the alloy Cunico. The lines can be described by the relationship

$$\ln H_c = A \ln \delta + B, \quad (1)$$

where the slope and intercept constants  $A$  and  $B$  have the following values for natural logarithms:

Alloy series	$A$	$B$	$I_s$
Fe-Ni-Al	1.48	9.48	1480
Cu-Ni-Co	1.15	7.13	1060
Ni-Au	0.45	4.37	432

It should be noted that the coefficients  $A$  and  $B$  decrease with saturation magnetization of the precipitate. The relationship is given graphically in Fig. 8, from which empirical evaluations of the coefficients are possible. From these, a general relationship expressing the data for the three series of alloys would be

$$\ln H_c = 0.00103 I_s \ln \delta + 0.005 I_s + 2. \quad (2)$$

It is interesting to compare the extrapolated values for zero packing, shown at the upper end of the curves in Fig. 6, with those for maximum disregistry (also zero packing) in the alloy series in Fig. 7. The latter give higher extrapolated values closer to those calculated for shape anisotropy. If it were possible to precipitate pure Fe with  $I_s = 1714$  coherent with NiAl ( $\delta = 0.42$ ), then according to the empirical expression (2) the coercive force would reach 8300 oersteds, compared with 5200 oersteds calculated for randomly oriented needle-like particles. Thus, there tends to be some reasonable agree-

<sup>3</sup> W. Köster and W. Dannöhl, Z. Metallk. 28, 248 (1936).

<sup>4</sup> W. Dannöhl and H. Neumann, Z. Metallk. 30, 218 (1938).

<sup>5</sup> S. Kuiti, Rept. Aero. Res. Inst. Tokyo Imperial University 15, 601 (1940).

<sup>†</sup> Saturation values for the equilibrium precipitates of compositions shown by the phase diagrams were obtained from the work of Marian (reference 6), Sucksmith (reference 7), and Dannöhl (reference 4). Maximum coercive force values are from the work of Köster (reference 3), Dannöhl (reference 4), and Geisler (references 1 and 9).

<sup>6</sup> V. Marian, Ann. phys. 7(11), 459 (1937).

<sup>7</sup> W. Sucksmith, Proc. Roy. Soc. (London) A171, 525 (1939).

<sup>8</sup> Bradley, Cox, and Goldschmidt, J. Inst. Metals 67, 189 (1941).

<sup>9</sup> A. H. Geisler and J. B. Newkirk, Trans. Am. Inst. Mining Met. Engrs. 180, 101 (1949).

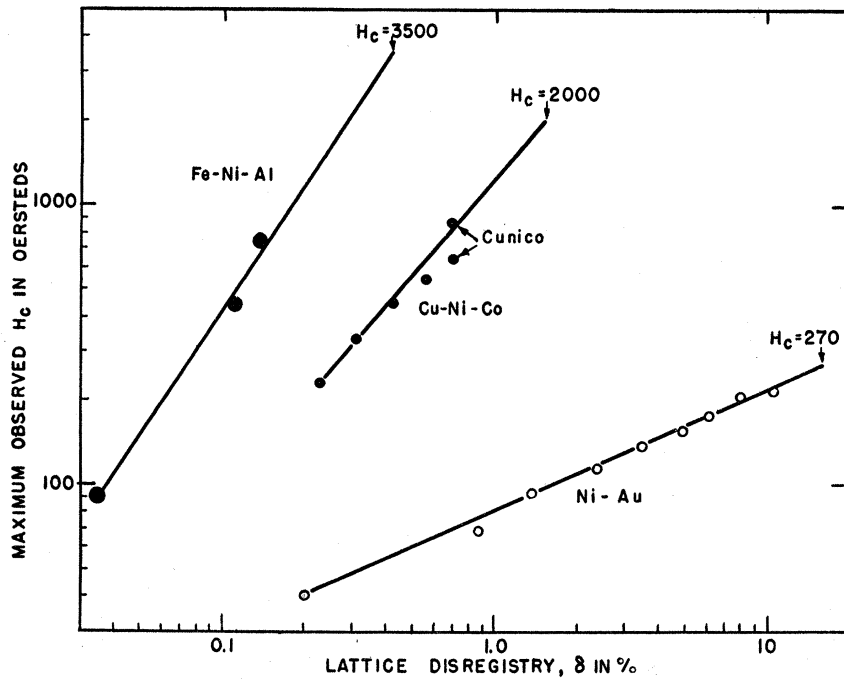


FIG. 7. Relation between maximum coercive force and precipitate disregistry or tetragonality.

ment of empirical and formal theory, regardless of the full magnitude difference when the comparison is made with the actually observed coercive forces of commercial alloys.

Attempts to fit the data for other alloys of the same type to the empirical expression are reasonably successful. The data given in Table I are based upon estimates of the composition and saturation magnetization of the precipitate phase in alloys with more than three components. The values of disregistry are based on lattice parameter measurements for the various alloys. The data are plotted in Fig. 9, where the line represents the relationship derived from the data for the three series of alloys. Cunife and the more complex Alnicos agree as well with the line as do Alnico 3, Cunico, and Au-30

percent Ni, alloys in the three series from which the expression was derived. Thus, it seems possible for the first time to justify the variation in coercive force among the commercial permanent magnet alloys of the simple precipitation type on the basis of fundamental properties of the precipitate: its saturation magnetization and its crystal lattice disregistry relative to the matrix. The relationship reconciles observations involving all three cubic ferromagnetic metals, Fe, Ni, and Co.

The role of disregistry in affecting the coercive force of fine precipitates could conceivably be threefold, involving all criteria which have been considered in the theory of the coercive force of fine particles.<sup>2</sup> In all three cases the effect is caused by low disregistry (under 10 percent), which promotes extensive coherent growth of the precipitate. First, disregistry will affect particle-shape anisotropy; for when disregistry is low, the particles can grow as coherent plates or needles, to keep surface energy low with minimum strain energy. Increasing disregistry would lead to decreasing shape anisotropy (inverse of desired relationship); for as the strain energy increases, coherency diminishes, and minimum surface energy requires a spherical shape. Second, higher disregistry leads to higher tetragonality at the coherent state, with an increased magnetic anisotropy of the precipitate. Third, the elastic strains for coherency entail high stresses, which increase to a limiting value with increasing disregistry. Since magnetostriction is not included, at least in the rough form of the empirical expression, it would seem that the third factor need not be considered. The first factor probably accounts for the direct dependence of coercive force on

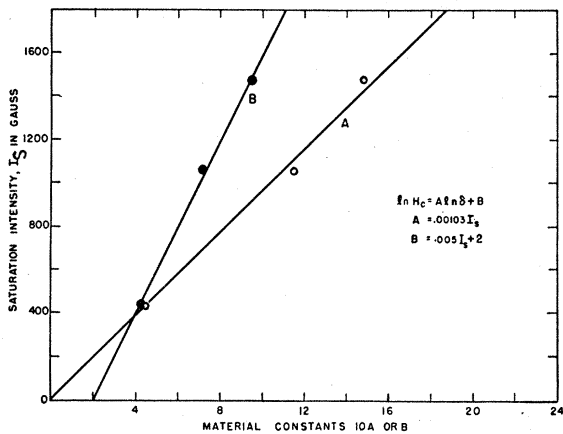


FIG. 8. Relation between intensity of magnetization at saturation and coefficients for the equations of curves in Fig. 7.

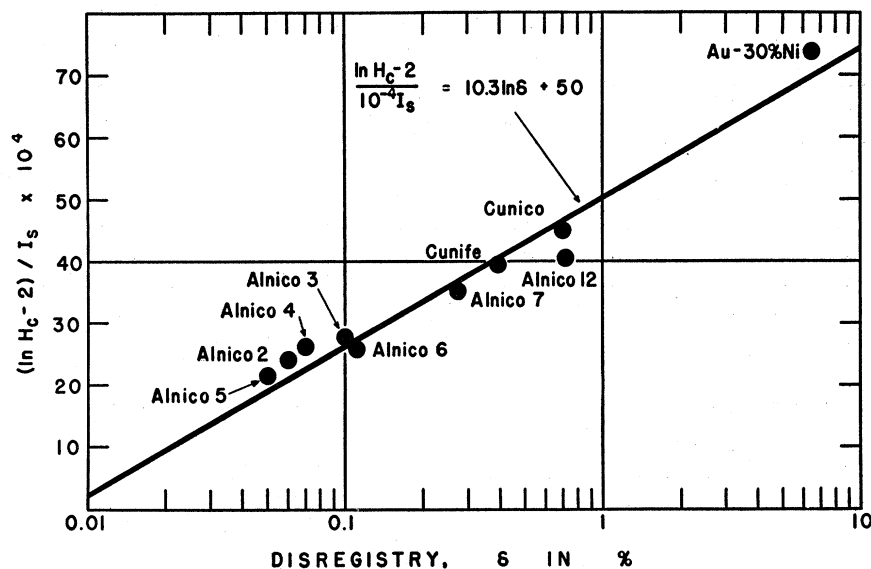


Fig. 9. Empirical relation for composition dependence of maximum coercive force, showing conformance of the commercial alloys and a Ni-Au alloy.

saturation magnetization as in theory; however, in the range of disregistry considered here the inverse relation to disregistry is not dominant. All of the alloys considered here have precipitate particles with appreciable shape anisotropy, 5 to 10 or more when the particles are large enough to resolve in the microscope. Thus, it would seem that the dominant role of disregistry is by means of its effect on crystal anisotropy. While absolute values were not considered, perhaps the expression is concerned only with the increasing magnetic anisotropy of a cubic lattice (a feature the alloys have in common) as tetragonality at the coherent state is increased. Evidence that this condition may be the case is found in the fact that the coefficients of Eq. (2) are not the same as those needed to explain the disregistry dependence of the coercive force of the CoPt type of ordering alloys, where the new phase at equilibrium may be tetragonal.

The departure of the calculated coercive forces listed in Table I from the observed could be attributed to deviation of the particle shape from the needle-like assumed for the theory. All the alloys have plate-like particles when of microscopically resolvable sizes, but it is known that a needle-like shape precedes the plate-like in some precipitation alloys. Correlation of coercive force with packing factor in Fig. 6 is based on the ultimate packing factor which obtains at complete equilibrium. This assumed value is probably greater than the value at maximum coercive force, where precipitation is only partly completed, and any correction would merely exaggerate the departure from calculated coercive force values. The saturation magnetization of the coherent precipitate was assumed to be that of the unstrained second phase at equilibrium. Although only a slight departure would be expected, it is appreciable in other cases such as the precipitation of iron from copper solid solutions.

While disregistry and ultimate packing appear to be

two factors which can be readily evaluated, it is possible that there are other less tangible factors which might explain the composition variation of coercive force in an alloy series. Other factors which cannot be readily evaluated quantitatively would include particle size and size distribution, which may be implicit in the condition for maximum observed coercive force. The time of the maximum in the aging curve is probably controlled by the attainment of an optimum size distribution and packing of the more ferromagnetic precipitate.† These features depend upon nucleation and growth rates of the precipitate, which in turn are related to the free energy change on precipitation. Since free energy change goes through a maximum near the middle of the miscibility gap in the phase diagram, the nucleation rate would be a maximum here, leading to the narrowest size distribu-

TABLE I. Properties of the precipitation type of permanent magnet alloys

Alloy	Approximate composition of precipitate	Precipitate $I_s$	$\delta$	Maximum coercive force observed	calculated <sup>b</sup>
Alnico 2	<sup>a</sup> Fe-15%Co-4%Ni-4%Al-3%Cu	1800 <sup>a</sup>	0.06	550	2450
Alnico 3	Fe-5%Ni-5%Al	1480	0.10	450	2010
Alnico 4	<sup>a</sup> Fe-10%Co-4%Ni-4%Al	1750 <sup>a</sup>	0.07	700	2380
Alnico 5	<sup>a</sup> Fe-30%Co-3%Ni-3%Al random <sup>c</sup>	1900 <sup>a</sup>	0.05	450	2620
Alnico 5DG	<sup>a</sup> Fe-30%Co-3%Ni-3%Al aligned	1900 <sup>a</sup>	0.05	640	5500
Alnico 6	<sup>a</sup> Fe-30%Co-3%Ni-3%Al-2%Ti	1780 <sup>a</sup>	0.11	750	2420
Alnico 7	<sup>a</sup> Fe-25%Co-4%Ni-4%Al-4%Ti	1500 <sup>a</sup>	0.28	1200	2040
Alnico 12	<sup>a</sup> Fe-20%Co-5%Ni-5%Al-6%Ti	1200 <sup>a</sup>	0.73	950	1630
Cunifo	Co-29%Ni-7%Cu	1060	0.70	870	1440
Cunife	Fe-40%Ni-10%Cu	1100 <sup>a</sup>	0.39	550	1500
Au-30%Ni	Ni-10%Au	432	6.51	180	590

<sup>a</sup> Estimated.

<sup>b</sup> Calculated for randomly oriented, needle-like particles with packing factor of 0.5,  $H_e = 1.36I_s$ .

<sup>c</sup> Without field treatment during cooling.

† In alloys rich in the ferromagnetic component, which would be the continuous phase upon completion of precipitation, the pertinent "precipitate" would be the small impoverished shells surrounding the particles of the nonmagnetic phase at the state of partial precipitation.

tion. Thus, if size distribution alone were the controlling factor, the coercive force—composition curve would be expected to exhibit an inverted U shape analogous to the solubility limit (Fig. 5) rather than the continuous rise towards the side rich in the less magnetic component.

#### SUMMARY

The coercive force of alloys such as Ni-Au, Cunico, Cunife, and the Alnicos is related directly to the saturation magnetization and disregistry of the precipitate. The latter factor is a measure of the degree of tetrago-

nality and strain which the precipitate must sustain to be coherent with the parent matrix at the state of high coercive force. Consideration of other factors such as the absolute magnitude of magnetic anisotropy, magnetostriction, and packing, which are incorporated in formal theories, seems unnecessary to rationalize the coercive force of these alloys.

It is hoped that this description of the various aspects of permanent magnet alloys will lead to an extension of the formal theory of fine particle magnets that will be applicable to the known alloys.

## The Physical and Magnetic Structure of the Mishima Alloys

E. A. NESBITT AND R. D. HEIDENREICH

*Bell Telephone Laboratories, Murray Hill, New Jersey*

THE Mishima alloys<sup>1</sup> of the iron-nickel-aluminum system, discovered in 1932, have been the subject of many structural and magnetic investigations

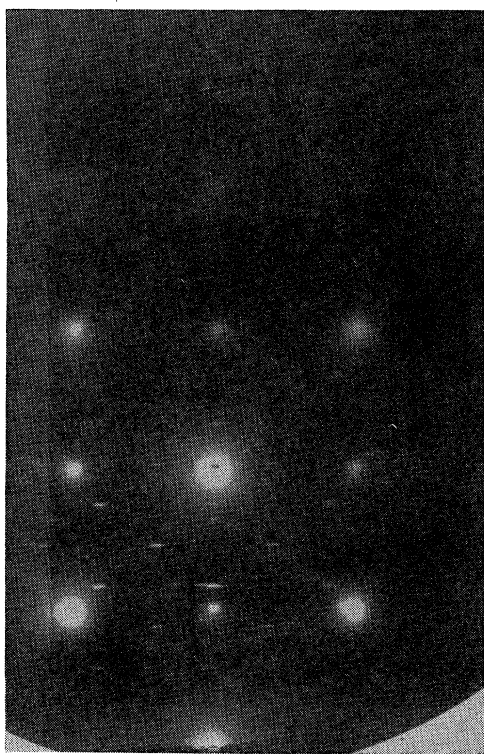


FIG. 1. Electron diffraction reflection pattern from Mishima single crystal (approx.  $\text{Fe}_2\text{NiAl}$ ). (100) surface and electron beam along (100) direction. Array of needle-like spots indicates permanent magnet precipitate. Crystal cooled from  $1300^\circ\text{C}$  at  $3^\circ\text{C}$  per second, then aged at  $600^\circ\text{C}$  for 1 hour.

<sup>1</sup> Mishima, *Stahl und Eisen* **53**, 79 (1933).

because of their interesting permanent magnet properties. Although a completely satisfactory equilibrium diagram has not yet evolved, many controversial points have been settled, and there has been substantial agreement by recent investigators<sup>2-4</sup> for the main reaction of the system. Because of these investigations, the permanent magnet properties have been attributed until now to a body-centered cubic precipitate which has approximately the same lattice spacing as its body-centered cubic matrix (2.86Å). According to Bradley and Taylor,<sup>5</sup> this precipitate lattice under permanent magnet conditions conforms to the dimensions of the parent lattice. The idea of two body-centered cubic lattices of approximately the same spacing was also extended to the case of Alnico 5 in order to explain the high coercive force in this alloy. However, as a result of the recent discovery of a new face-centered cubic precipitate<sup>6</sup> in Alnico 5, which was found to be the agent responsible for the alloy's permanent magnet properties, it was decided to re-investigate the cause of the permanent magnet properties in the Mishima alloys.

Figure 1 shows an electron diffraction pattern obtained on a (100) single crystal (approximately  $\text{Fe}_2\text{NiAl}$ ) cooled from  $1300^\circ\text{C}$  at  $3^\circ\text{C}$  per second and aged at  $600^\circ\text{C}$  for 1 hour. The intense spots are those due to the body-centered cubic structure, and the less intense spots are superlattice reflections indicating that the alloy is ordered. The array of needle-like spots in this photograph

<sup>2</sup> A. J. Bradley and A. Taylor, *Proc. Royal Soc. (London)* **166A**, 353 (1938).

<sup>3</sup> S. Kiuti, *Japan Nickel Rev.* **9**, 78 (1941).

<sup>4</sup> W. Dannohl, *Arch. Eisenhüttenw.* **15**, 321 (1942).

<sup>5</sup> A. J. Bradley and A. Taylor, *Physics in Industry*, "Magnetism" (Institute of Physics, London, 1938), p. 91.

<sup>6</sup> R. D. Heidenreich and E. A. Nesbitt, *J. Appl. Phys.* **23**, 352 (1952); E. A. Nesbitt and R. D. Heidenreich, *J. Appl. Phys.* **23**, 366 (1952).

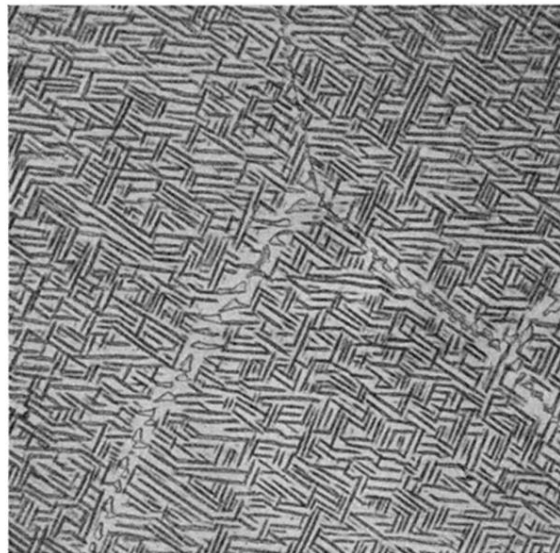


FIG. 1. Microstructure of Alnico 2 showing plate-like precipitate of resolvable particles larger than those responsible for high coercive force. 1000X.